(Invitrogen), followed by limiting dilution cloning, S6.2 and BOS-5 clones were obtained. To detect S protein expression in S6.2 cells, the cells were stained with biotinylated anti-S monoclonal antibody (Ohnishi et al., 2005) or control antibody, followed by the incubation with APC-streptavidin (e-Bioscience Inc., San Diego, CA), after which they were analyzed by FACScalibur (BD Bioscience) using the Cell Quest II program. Propidium Iodide was used to exclude dead cells. The data were re-analyzed and depicted using Flowjo software (Tree Star Inc., San Carlos, CA).

ELISPOT assay. Spleen T cells of mice immunized with rDIsSARS-N or rDIsSARS-E/M/N/S were separated using a MACS system (Miltenyi Biotec, Auburn, CA). To enrich $CD4^+$ T cells in the T cell fraction, $CD8^+$ T cells were partially removed using anti-CD8 mAb-coated magnetic beads (Miltenyi Biotec). This procedure reduced the number of $CD8^+$ T cells to less than one third. Overlapping 20-mer peptides covering the whole N sequences of SARS-CoV were obtained from Sigma-Aldrich Japan. S peptides S44 (S331-350), S45 (S381-400), S46 (S431-450), and S47 (S481-500) corresponding to the ACE2 binding region of the S protein were selectively produced based on a web-site program by SYFPEITHI (http://syfpeithi.de/). A20.2J murine B cells irradiated at 2000 cGy were used as APCs with peptides corresponding to either S or N proteins. In some experiments, A20.2J cells stably transfected with pEF-S or the empty vector pEF-BOS were used.

ELISPOT assays were performed according to the methods outlined by DIACLONE research (Besancon, France). In brief, 96-well flat-bottom plates (Maxisoap Nunc plates, Nunc, Rochester, NY) were coated with anti-IFN-γ capture antibody for one hour at

37°C. The plates were then washed with PBS containing 0.05% Tween 20 (PBST), and blocked with PBS containing 2% bovine serum albumin overnight at 4°C. Freshly isolated splenic T cells ($5x10^5$) and APCs ($1x10^4$) were added to the plates in the presence or absence of 5 μM of N or S peptides and incubated for 16 hr at 37°C in 5% CO_2 on the anti-IFN-γ-coated plates, followed by a lysis with ice-cold de-ionized water. After the plates were washed, biotinylated detection antibody was added, then the plates were further incubated for 1 hr at 37°C. The plates were washed three times with PBST, then 50 μl/well of Streptavidin-alkaline phosphatase-conjugated anti-biotin immunoglobulin G solution was added, followed by incubation for 1 h at 37°C. After washing with PBST, substrate mix (50 μl/well) was added, and the plates were allowed to develop over four hours at 37°C. The wells were imaged and the number of spot-forming cells SFC counted using a KS ELISPOT compact system (Carl Zeiss, Jena, Germany).

Histopathology and immunohistochemistry. Lung tissue from the mice was fixed in 10% buffered formalin and embedded in paraffin. Paraffin block sections were stained with hematoxylin and eosin (HE). SARS-CoV antigens were immunohistochemically detected using a labeled-streptoavidin-biotin complex staining system (DakoCytomation Co. Japan, Kyoto, Japan). Rabbit polyclonal antibodies raised against UV-inactivated, purified SARS-CoV were used as a primary antibody. A catalyzed signal amplification method (Dako) was also used to detect SARS-CoV antigens with enhanced sensitivity. Lung sections from mice vaccinated with rDIsSARS-E/M/N/S and infected with SARS Co-V were stained with anti-CD3 antibody. (Santa Cruz Biotechnology)

Acknowledgments

We would like to thank Dr. Michinori Kohara for kindly providing us anti-SARS-CoV polyclonal antibodies. We would also like to thank Ms. Mami Matsuda, Ms. Makiko Yahata, Ms. Sayaka Yoshizaki, Ms. Chikako Sato, Mr. Masayuki Ishige, Ms. Yuko Sato and Ms. Aya Harashima for their excellent technical support. This study was supported by a Heath and Labour Science Research Grant from the Ministry of Health, Labour, and Welfare, Japan.

References

Anton, I. M., Gonzalez, S., Bullido, M. J., Corsin, M., Risco, C., Langeveld, J. P., and Enjuanes, L. (1996). Cooperation between transmissible gastroenteritis coronavirus (TGEV) structural proteins in the in vitro induction of virus-specific antibodies. *Virus Res* **46**(1-2), 111-24.

Belyakov, I. M., Wyatt, L. S., Ahlers, J. D., Earl, P., Pendleton, C. D., Kelsall, B. L., Strober, W., Moss, B., and Berzofsky, J. A. (1998). Induction of a mucosal cytotoxic T-lymphocyte response by intrarectal immunization with a replication-deficient recombinant vaccinia virus expressing human immunodeficiency virus 89.6 envelope protein. *J. Virol.* **72**, 8264-8272.

Bisht, H., Roberts, A., Vogel, L., Bukreyev, A., Collins, P. L., Murphy, B. R., Subbarao, K., and Moss, B. (2004). Severe acute respiratory syndrome coronavirus spike protein expressed by attenuated vaccinia virus protectively immunizes mice. *Proc Natl Acad Sci U S A* **101**(17), 6641-6.

Buchholz, U. J., Bukreyev, A., Yang, L., Lamirande, E. W., Murphy, B. R., Subbarao, K., and Collins, P. L. (2004). Contributions of the structural proteins of severe acute respiratory syndrome coronavirus to protective immunity. *Proc Natl Acad Sci U S A* **101**(26), 9804-9.

Bukreyev, A., Lamirande, E. W., Buchholz, U. J., Vogel, L. N., Elkins, W. R., St Claire, M., Murphy, B. R., Subbarao, K., and Collins, P. L. (2004). Mucosal immunisation of African green monkeys (Cercopithecus aethiops) with an attenuated parainfluenza virus expressing the SARS coronavirus spike protein for the prevention of SARS. *Lancet* **363**(9427), 2122-7.

Collins, A. R., Knobler, R. L., Powell, H., and Buchmeier, M. J. (1982). Monoclonal antibodies to murine hepatitis virus-4 (strain JHM) define the viral glycoprotein responsible for attachment and cell--cell fusion. *Virology* **119**(2), 358-71.

Collisson, E. W., Pei, J., Dzielawa, J., and Seo, S. H. (2000). Cytotoxic T lymphocytes are critical in the control of infectious bronchitis virus in poultry. *Dev Comp Immunol* **24**(2-3), 187-200.

Czub, M., Weingartl, H., Czub, S., He, R., and Cao, J. (2005). Evaluation of modified vaccinia virus Ankara based recombinant SARS vaccine in ferrets. *Vaccine* **23**(17-18), 2273-9.

Drosten, C., Gunther, S., Preiser, W., van der Werf, S., Brodt, H. R., Becker, S., Rabenau, H., Panning, M., Kolesnikova, L., Fouchier, R. A., Berger, A., Burguiere, A. M., Cinatl, J., Eickmann, M., Escriou, N., Grywna, K., Kramme, S., Manuguerra, J. C., Muller, S., Rickerts, V., Sturmer, M., Vieth, S., Klenk, H. D., Osterhaus, A. D., Schmitz, H., and Doerr, H. W. (2003). Identification of a novel coronavirus in patients with severe acute respiratory syndrome. *N Engl J Med* **348**(20), 1967-76.

Faber, M., Lamirande, E. W., Roberts, A., Rice, A. B., Koprowski, H., Dietzschold, B., and Schnell, M. J. (2005). A single immunization with a rhabdovirus-based vector expressing severe acute respiratory syndrome coronavirus (SARS-CoV) S protein results in the production of high levels of SARS-CoV-neutralizing antibodies. *J Gen Virol* **86**(Pt 5), 1435-40.

Falkner, F. G., and Moss, B. (1988). Escherichia coli gpt gene provides dominant selection for vaccinia virus open reading frame expression vectors. *J Virol* **62**(6), 1849-54.

Fouchier, R. A., Kuiken, T., Schutten, M., van Amerongen, G., van Doornum, G. J., van den Hoogen, B. G., Peiris, M., Lim, W., Stohr, K., and Osterhaus, A. D. (2003). Aetiology: Koch's postulates fulfilled for SARS virus. *Nature* **423**(6937), 240.

Gao, W., Tamin, A., Soloff, A., D'Aiuto, L., Nwanegbo, E., Robbins, P. D., Bellini, W. J., Barratt-Boyes, S., and Gambotto, A. (2003). Effects of a SARS-associated coronavirus vaccine in monkeys. *Lancet* **362**(9399), 1895-6.

Groneberg, D. A., Poutanen, S. M., Low, D. E., Lode, H., Welte, T., and Zabel, P. (2005). Treatment and vaccines for severe acute respiratory syndrome. *Lancet Infect Dis* **5**(3), 147-55.

Holmes, K. V. (2003). SARS coronavirus: a new challenge for prevention and therapy. *J Clin Invest* **111**(11), 1605-9.

Ichinohe, T., Watanabe, I., Ito, S., Fujii, H., Moriyama, M., Tamura, S., Takahashi, H., Sawa, H., Chiba, J., Kurata, T., Sata, T., and Hasegawa, H. (2005). Synthetic double-stranded RNA poly(I:C) combined with mucosal vaccine protects against influenza virus infection. *J Virol* **79**(5), 2910-9.

Ishii, K., Ueda, Y., Matsuo, K., Matsuura, Y., Kitamura, T., Kato, K., Izumi, Y., Someya, K., Ohsu, T., Honda, M., and Miyamura, T. (2002). Structural analysis of vaccinia virus DIs strain: application as a new replication-deficient viral vector.

Virology **302**(2), 433-44.

Jackwood, M. W., and Hilt, D. A. (1995). Production and immunogenicity of multiple antigenic peptide (MAP) constructs derived from the S1 glycoprotein of infectious bronchitis virus (IBV). *Adv Exp Med Biol* **380**, 213-9.

Kapadia, S. U., Rose, J. K., Lamirande, E., Vogel, L., Subbarao, K., and Roberts, A. (2005). Long-term protection from SARS coronavirus infection conferred by a single immunization with an attenuated VSV-based vaccine. *Virology*.

Kim, T. W., Lee, J. H., Hung, C. F., Peng, S., Roden, R., Wang, M. C., Viscidi, R., Tsai, Y. C., He, L., Chen, P. J., Boyd, D. A., and Wu, T. C. (2004). Generation and characterization of DNA vaccines targeting the nucleocapsid protein of severe acute respiratory syndrome coronavirus. *J Virol* **78**(9), 4638-45.

Kitamura, T., Kitamura, T., and Tagaya, I. (1967). Immunogenicity of an attenuated strain of vaccinia virus on rabbits and monkeys. *Nature* **215**, 1187-1188.

Ksiazek, T. G., Erdman, D., Goldsmith, C. S., Zaki, S. R., Peret, T., Emery, S., Tong, S., Urbani, C., Comer, J. A., Lim, W., Rollin, P. E., Dowell, S. F., Ling, A. E., Humphrey, C. D., Shieh, W. J., Guarner, J., Paddock, C. D., Rota, P., Fields, B., DeRisi, J., Yang, J. Y., Cox, N., Hughes, J. M., LeDuc, J. W., Bellini, W. J., and Anderson, L. J. (2003). A novel coronavirus associated with severe acute respiratory syndrome. *N Engl J Med* **348**(20), 1953-66.

Li, W., Moore, M. J., Vasilieva, N., Sui, J., Wong, S. K., Berne, M. A., Somasundaran, M., Sullivan, J. L., Luzuriaga, K., Greenough, T. C., Choe, H., and Farzan, M. (2003). Angiotensin-converting enzyme 2 is a functional receptor for the SARS coronavirus. *Nature* **426**(6965), 450-4.

Marra, M. A., Jones, S. J., Astell, C. R., Holt, R. A., Brooks-Wilson, A., Butterfield, Y. S., Khattra, J., Asano, J. K., Barber, S. A., Chan, S. Y., Cloutier, A., Coughlin, S. M., Freeman, D., Girn, N., Griffith, O. L., Leach, S. R., Mayo, M., McDonald, H., Montgomery, S. B., Pandoh, P. K., Petrescu, A. S., Robertson, A. G., Schein, J. E., Siddiqui, A., Smailus, D. E., Stott, J. M., Yang, G. S., Plummer, F., Andonov, A., Artsob, H., Bastien, N., Bernard, K., Booth, T. F., Bowness, D., Czub, M., Drebot, M., Fernando, L., Flick, R., Garbutt, M., Gray, M., Grolla, A., Jones, S., Feldmann, H., Meyers, A., Kabani, A., Li, Y., Normand, S., Stroher, U., Tipples, G. A., Tyler, S., Vogrig, R., Ward, D., Watson, B., Brunham, R. C., Krajden, M., Petric, M., Skowronski, D. M., Upton, C., and Roper, R. L. (2003).

The Genome sequence of the SARS-associated coronavirus. *Science* **300**(5624), 1399-404.

Meeusen, E. N., Scheerlinck, J. P., Wattegedera, S., and Entrican, G. (2004). Advances in mucosal vaccination. *Anim Health Res Rev* **5**(2), 209-17.

Mizutani, T., Fukushi, S., Saijo, M., Kurane, I., and Morikawa, S. (2004). Phosphorylation of p38 MAPK and its downstream targets in SARS coronavirus-infected cells. *Biochem Biophys Res Commun* **319**(4), 1228-34.

Nal, B., Chan, C., Kien, F., Siu, L., Tse, J., Chu, K., Kam, J., Staropoli, I., Crescenzo-Chaigne, B., Escriou, N., van der Werf, S., Yuen, K. Y., and Altmeyer, R. (2005). Differential maturation and subcellular localization of severe acute respiratory syndrome coronavirus surface proteins S, M and E. *J Gen Virol* **86**(Pt 5), 1423-34.

Nam, J. H., Wyatt, L. S., Chae, S. L., Cho, H. W., Park, Y. K., and Moss, B. (1999). Protection against lethal Japanese encephalitis virus infection of mice by immunization with the highly attenuated MVA strain of vaccinia virus expressing JEV prM and E genes. *Vaccine* **17**(3), 261-268.

Ohnishi, K., Sakaguchi, M., Kaji, T., Akagawa, K., Taniyama, T., Kasai, M., Tsunetsugu-Yokota, Y., Oshima, M., Yamamoto, K., Takasuka, N., Hashimoto, S., Ato, M., Fujii, H., Takahashi, Y., Morikawa, S., Ishii, K., Sata, T., Takagi, H., Itamura, S., Odagiri, T., Miyamura, T., Kurane, I., Tashiro, M., Kurata, T., Yoshikura, H., and Takemori, T. (2005). Immunological detection of severe acute respiratory syndrome coronavirus by monoclonal antibodies. *Jpn J Infect Dis* **58**(2), 88-94.

Peiris, J. S., Lai, S. T., Poon, L. L., Guan, Y., Yam, L. Y., Lim, W., Nicholls, J., Yee, W. K., Yan, W. W., Cheung, M. T., Cheng, V. C., Chan, K. H., Tsang, D. N., Yung, R. W., Ng, T. K., and Yuen, K. Y. (2003). Coronavirus as a possible cause of severe acute respiratory syndrome. *Lancet* **361**(9366), 1319-25.

Rota, P. A., Oberste, M. S., Monroe, S. S., Nix, W. A., Campagnoli, R., Icenogle, J. P., Penaranda, S., Bankamp, B., Maher, K., Chen, M. H., Tong, S., Tamin, A., Lowe, L., Frace, M., DeRisi, J. L., Chen, Q., Wang, D., Erdman, D. D., Peret, T. C., Burns, C., Ksiazek, T. G., Rollin, P. E., Sanchez, A., Liffick, S., Holloway, B., Limor, J., McCaustland, K., Olsen-Rasmussen, M., Fouchier, R., Gunther, S., Osterhaus, A. D., Drosten, C., Pallansch, M. A., Anderson, L. J., and Bellini, W.

J. (2003). Characterization of a novel coronavirus associated with severe acute respiratory syndrome. *Science* **300**(5624), 1394-9.

Ruan, Y. J., Wei, C. L., Ee, A. L., Vega, V. B., Thoreau, H., Su, S. T., Chia, J. M., Ng, P., Chiu, K. P., Lim, L., Zhang, T., Peng, C. K., Lin, E. O., Lee, N. M., Yee, S. L., Ng, L. F., Chee, R. E., Stanton, L. W., Long, P. M., and Liu, E. T. (2003). Comparative full-length genome sequence analysis of 14 SARS coronavirus isolates and common mutations associated with putative origins of infection. *Lancet* **361**(9371), 1779-85.

Seo, S. H., Wang, L., Smith, R., and Collisson, E. W. (1997). The carboxyl-terminal 120-residue polypeptide of infectious bronchitis virus nucleocapsid induces cytotoxic T lymphocytes and protects chickens from acute infection. *J Virol* **71**(10), 7889-94.

Someya, K., Xin, K. Q., Matsuo, K., Okuda, K., Yamamoto, N., and Honda, M. (2004). A consecutive priming-boosting vaccination of mice with simian immunodeficiency virus (SIV) gag/pol DNA and recombinant vaccinia virus strain DIs elicits effective anti-SIV immunity. *J Virol* **78**(18), 9842-53.

Stittelaar, K. J., Wyatt, L. S., de Swart, R. L., Vos, H. W., Groen, J., van Amerongen, G., van Binnendijk, R. S., Rozenblatt, S., Moss, B., and Osterhaus, A. D. (2000). Protective immunity in macaques vaccinated with a modified vaccinia virus Ankara-based measles virus vaccine in the presence of passively acquired antibodies. *J. Virol.* **74**, 4236-4243.

Storch, G. A. (2001). Diagnostic Virology. 4th ed. *In* "Fields Virology" (P. M. H. David M Knipe, Ed.), pp. 493-531. Lippincott Williams & Wilkins, Philadelphia, PA.

Subbarao, K., McAuliffe, J., Vogel, L., Fahle, G., Fischer, S., Tatti, K., Packard, M., Shieh, W. J., Zaki, S., and Murphy, B. (2004). Prior infection and passive transfer of neutralizing antibody prevent replication of severe acute respiratory syndrome coronavirus in the respiratory tract of mice. *J Virol* **78**(7), 3572-7.

Sutter, G., and Moss, B. (1992). Nonreplicating vaccinia vector efficiently expresses recombinant genes. *Proc. Natl. Acad. Sci. USA* **89**, 10847-10851.

Sutter, G., Wyatt, L. S., Foley, P. L., Bennink, J. R., and Moss, B. (1994). A recombinant vector derived from the host range-restricted and highly attenuated MVA strain of vaccinia virus stimulates protective immunity in mice to influenza virus. *Vaccine* **12**, 1032-1040.

Tagaya, I., Kitamura, T., and Sano, Y. (1961). A new mutant of dermovaccinia virus. *Nature* **192**, 381-2.

Takasuka, N., Fujii, H., Takahashi, Y., Kasai, M., Morikawa, S., Itamura, S., Ishii, K., Sakaguchi, M., Ohnishi, K., Ohshima, M., Hashimoto, S., Odagiri, T., Tashiro, M., Yoshikura, H., Takemori, T., and Tsunetsugu-Yokota, Y. (2004). A subcutaneously injected UV-inactivated SARS coronavirus vaccine elicits systemic humoral immunity in mice. *Int Immunol* **16**(10), 1423-30.

Weingartl, H., Czub, M., Czub, S., Neufeld, J., Marszal, P., Gren, J., Smith, G., Jones, S., Proulx, R., Deschambault, Y., Grudeski, E., Andonov, A., He, R., Li, Y., Copps, J., Grolla, A., Dick, D., Berry, J., Ganske, S., Manning, L., and Cao, J. (2004). Immunization with modified vaccinia virus Ankara-based recombinant vaccine against severe acute respiratory syndrome is associated with enhanced hepatitis in ferrets. *J Virol* **78**(22), 12672-6.

Weisz, O. A., Swift, A. M., and Machamer, C. E. (1993). Oligomerization of a membrane protein correlates with its retention in the Golgi complex. *J Cell Biol* **122**(6), 1185-96.

Wyatt, L. S., Shors, S. T., Murphy, B. R., and Moss, B. (1996). Development of a replication-deficient recombinant vaccinia virus vaccine effective against parainfluenza virus 3 infection in an animal model. *Vaccine* **14**(15), 1451-8.

Xiao, X., Chakraborti, S., Dimitrov, A. S., Gramatikoff, K., and Dimitrov, D. S. (2003). The SARS-CoV S glycoprotein: expression and functional characterization. *Biochem Biophys Res Commun* **312**(4), 1159-64.

Yang, Z. Y., Kong, W. P., Huang, Y., Roberts, A., Murphy, B. R., Subbarao, K., and Nabel, G. J. (2004). A DNA vaccine induces SARS coronavirus neutralization and protective immunity in mice. *Nature* **428**(6982), 561-4.

Yang, Z. Y., Werner, H. C., Kong, W. P., Leung, K., Traggiai, E., Lanzavecchia, A., and Nabel, G. J. (2005). Evasion of antibody neutralization in emerging severe acute respiratory syndrome coronaviruses. *Proc Natl Acad Sci U S A* **102**(3), 797-801.

Yoshizawa, I., Soda, Y., Mizuochi, T., Yasuda, S., Rizvi, T. A., Takemori, T., and Tsunetsugu-Yokota, Y. (2001). Enhancement of mucosal immune response against HIV-1 Gag by DNA immunization. *Vaccine* **19**(20-22), 2995-3003.

You, J., Dove, B. K., Enjuanes, L., DeDiego, M. L., Alvarez, E., Howell, G., Heinen, P., Zambon, M., and Hiscox, J. A. (2005). Subcellular localization of the severe

acute respiratory syndrome coronavirus nucleocapsid protein. *J Gen Virol* **86**(Pt 12), 3303-10.

Zakhartchouk, A. N., Viswanathan, S., Mahony, J. B., Gauldie, J., and Babiuk, L. A. (2005). Severe acute respiratory syndrome coronavirus nucleocapsid protein expressed by an adenovirus vector is phosphorylated and immunogenic in mice. *J Gen Virol* **86**(Pt 1), 211-5.

Zhao, P., Cao, J., Zhao, L. J., Qin, Z. L., Ke, J. S., Pan, W., Ren, H., Yu, J. G., and Qi, Z. T. (2005). Immune responses against SARS-coronavirus nucleocapsid protein induced by DNA vaccine. *Virology* **331**(1), 128-35.

Zhi, Y., Kobinger, G. P., Jordan, H., Suchma, K., Weiss, S. R., Shen, H., Schumer, G., Gao, G., Boyer, J. L., Crystal, R. G., and Wilson, J. M. (2005). Identification of murine CD8 T cell epitopes in codon-optimized SARS-associated coronavirus spike protein. *Virology* **335**(1), 34-45.

Zhu, M. S., Pan, Y., Chen, H. Q., Shen, Y., Wang, X. C., Sun, Y. J., and Tao, K. H. (2004). Induction of SARS-nucleoprotein-specific immune response by use of DNA vaccine. *Immunol Lett* **92**(3), 237-43.

Figure Legends

Fig.1. Schematic diagram of rDIs constructs expressing SARS-CoV structural proteins. DNA fragments encoding E, M, N and S proteins were inserted into the location of the 15.4 kb deletion in DIs using the vaccinia virus transfer vector pDIsgptmH5. Six rDIs constructs are shown.

Fig.2. Western blot analysis and indirect immunofluorescence analysis.

A: CEF cells were infected with rDIs constructs expressing SARS-CoV structural proteins (M, N and S, respectively). Purified SARS-CoV virion (0.5 mg) was used as a positive control. SARS-CoV proteins were detected using monoclonal antibodies (N and S) or polyclonal antibodies (M). Detection of bound antibodies was done with horseradish peroxidase-conjugated goat anti-mouse or anti-rabbit antibody, and visualized by chemiluminescence.

B: CEF cells were infected with rDIs constructs expressing SARS-CoV structural proteins (M, N and S, respectively). To detect SARS-CoV proteins, the cells were incubated with rabbit polyclonal antibodies against these proteins. The cells were further incubated with FITC-conjugated goat anti-rabbit IgG. To analyze subcellular localization of these proteins, monoclonal antibody against GM-130 (Golgi marker) and rhodamine-conjugated goat anti-mouse IgG were used. SARS proteins are shown in green, Golgi apparatus is shown in red and co-localization, where it occurs, is shown in yellow.

Fig. 3. Detection of anti-SARS-CoV IgG in vaccinated mice.

IgG antibody levels against SARS-CoV were determined as described in the materials and methods section. SARS-CoV-specific IgG titers were calculated as follows: SARS-specific IgG titer (ELISA units/ml) = (the unit value obtained for wells coated with virus-infected cell lysate) - (the unit value obtained for wells coated with non-infected cell lysate). *: $p<0.1$, **: $p<0.05$, ***: $p<0.01$ vs. DIs-administered group. The data for neutralizing sera are represented by closed circles and the data for non-neutralizing sera are represented by open circles.

Fig. 4. Mucosally secreted anti-SARS-CoV IgG, but not IgA, antibodies are protective from nasal SARS-CoV challenge in vaccinated mice.

The levels of Ig A and IgG antibodies against SARS-CoV were determined as described in the materials and methods section. Fig. 4(A): Titers of anti-SARS-CoV IgA in the nasal washings of vaccinated mice. Error bars represent the mean +/- SD. Fig. 4(B): Titers of anti-SARS-CoV IgG in the nasal washings of vaccinated mice. Error bars represent the mean +/- SD. Fig. 4(C): Titers of anti-SARS-CoV IgG in the sera of vaccinated mice. Error bars represent the mean +/- SD. Fig. 4(D): The titers of SARS-CoV in the lungs of vaccinated mice challenged one week later with 10^4 $TCID_{50}$ of SARS-CoV. Virus titers are expressed as $\log_{10}TCID_{50}$. Error bars represent the mean +/- SD. *: $p<0.1$, **: $p<0.05$, ***: $p<0.01$ vs. DIs-administered group.

Fig. 5. In vitro response of SARS-CoV-specific T cells in mice subcutaneously immunized with rDIsSARS-S.

CLN, ALN and spleens were obtained from mice one week after the third vaccination of

either DIs control or rDIsSARS-S. After preparation of single cell suspensions, T cells were purified and cultivated with irradiated and T-cell depleted normal BALB/c mouse splenocytes as APCs in the presence or absence of 10 μg/ml of purified UV-irradiated SARS-CoV virion. Four days later, IFN-γ and TNF-α concentrations in the culture supernatant were measured.

Fig. 6. Detection of SARS-CoV-specific T cells elicited by rDIsSARS-E/M/N/S or rDIsSARS-N vaccination.

Splenic and lymph node (LN) T cells of mice s.c. or i.n. immunized with recombinant rDIsSARS-E/M/N/S (A) or rDIsSARS-N (B) were separated using a MACS system (Miltenyi Biotec), and IFN-γ ELISPOT analysis was performed.

A: T cells ($5x10^5$ cells) from mice immunized with rDIsSARS-E/M/N/S were cultured with irradiated A20.2J B cells ($1x10^4$), in triplicate, in a 96-well membrane plates coated with IFN-γ capture antibody in the absence or presence of 5 μM of S peptides (S44~S47). The numbers of IFN-γ spot-forming cells were then counted and are depicted.

B: T cells from mice immunized with rDIsSARS-N and A20.2J B cells were cultured as described in A. N protein (422 amino acids) was divided into 5 parts by 100 amino acids (A, B, C, D and E) and 10 peptides each of pooled 20-mer overlapping peptides specific to the each stretch of N sequence were used as an antigen.

Fig. 7. Detection of SARS-CoV S-specific $CD8^+$ T cells in mice immunized with rDIsSARS-E/M/N/S.

A: A20.2J B cell clone expressing S (S6.2) or empty vector (BOS-5) was stained with

biotinylated anti-SARS-CoV S monoclonal antibody (solid line) or control IgG (shadowed line), followed by the incubation with streptavidin-APC, and then analyzed by FACScalibur. A histogram of APC fluorescence of gated live cells (PI negative) is depicted.

B: Splenic T cells from mice immunized s.c. or i.n. with recombinant rDIsSARS-E/M/N/S were purified and IFN-γ ELISPOT analysis was carried out using γ-irradiated S6.2 and BOS-5 as APCs. The number of T cells reactive for BOS-5 control (white column) and S6.2 (black column) cells are shown. Error bars represent the mean +/- SD.

C: Using the same splenic T cells as in B, $CD8^+$ T cells were partially removed using anti-CD8 mAb-coated magnetic beads (Miltenyi Biotec), and the number of T cells reactive for BOS-5 and S6.2 cells were counted by ELISPOT. The number of BOS-5-reactive T cells was subtracted and the number of S-specific T cells is depicted. Black columns: total T cells; grey columns: partially CD8-depleted T cells.

Fig . 8. Histopathology and immunohistochemistry.

Lung specimen of mice immunized with rDIs expressing structural proteins of SARS-CoV and challenged with SARS-CoV. Mice were immunized i.n. or s.c. with DIs, rDIsSARS-N, rDIsSARS-E/M/S, rDIsSARS-E/M/N/S or saline. Mice were challenged with SARS-CoV 2 weeks after the final vaccination. Lungs were harvested 3 days after the challenge. The section was stained with hematoxylin and eosin (H&E) or immunohistochmically stained with anti-SARS-CoV antibody or anti-CD3 antibody.

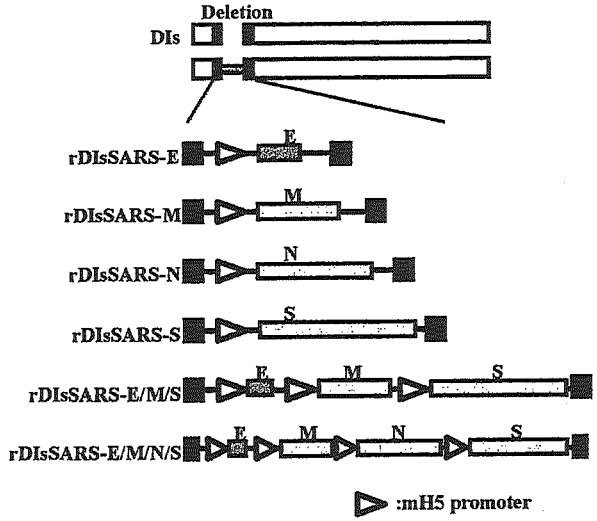
Deletion
DIs
rDIsSARS-E
E
rDIsSARS-M
M
rDIsSARS-N
N
rDIsSARS-S
S
rDIsSARS-E/M/S
E
M
S
rDIsSARS-E/M/N/S
E
M
N
S
:mH5 promoter

Fig.1

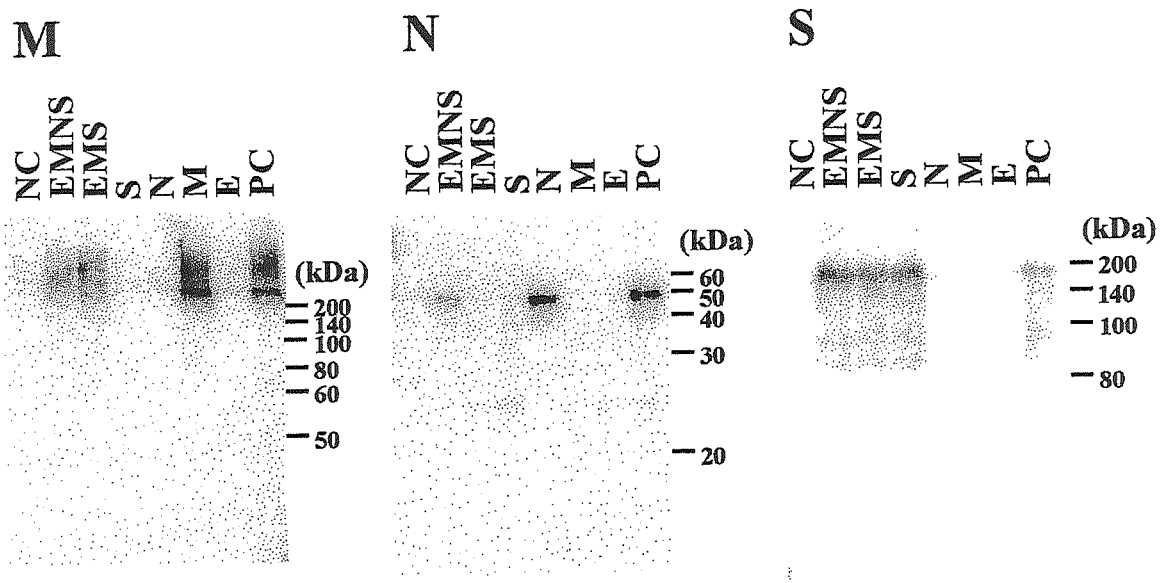
M
NC
EMNS
EMS
S
N
M
E
PC
(kDa)
200
140
100
80
60
50
N
NC
EMNS
EMS
S
N
M
E
PC
(kDa)
60
50
40
30
20
S
NC
EMNS
EMS
S
N
M
E
PC
(kDa)
200
140
100
80

Fig.2A

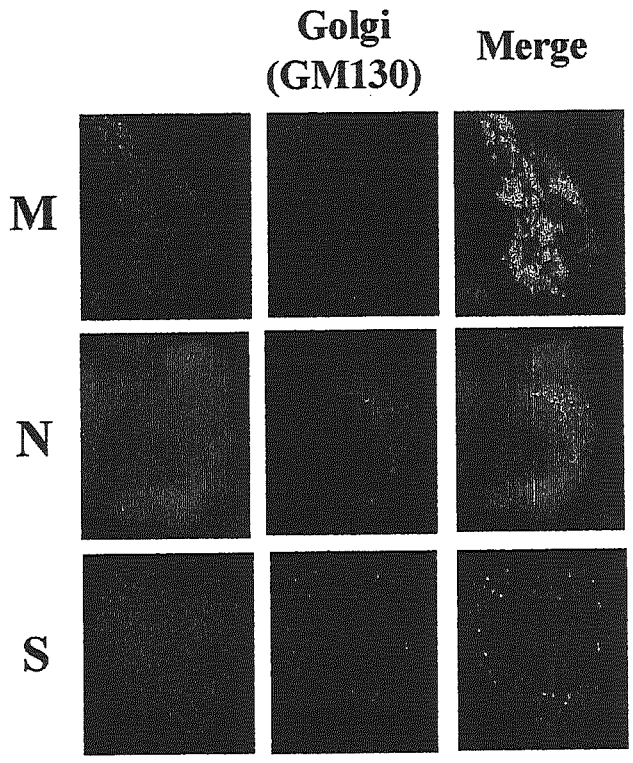

Fig.2B

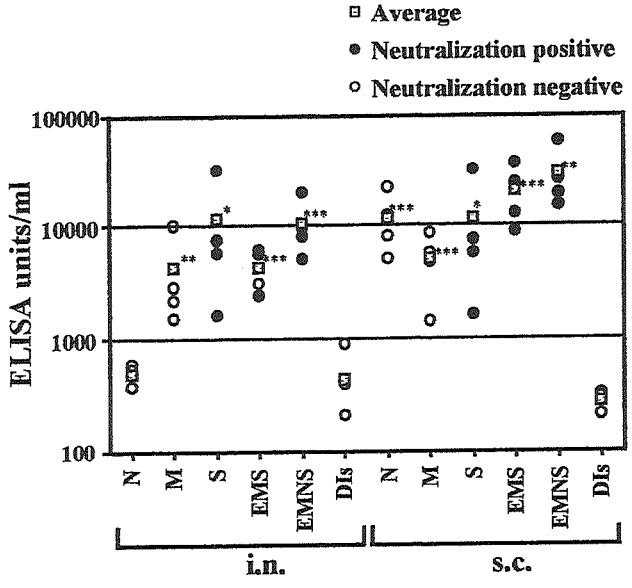
Average
Neutralization positive
Neutralization negative
ELISA units/ml
100000
10000
1000
100
N
M
S
EMS
EMNS
DIs
i.n.
s.c.

Fig.3

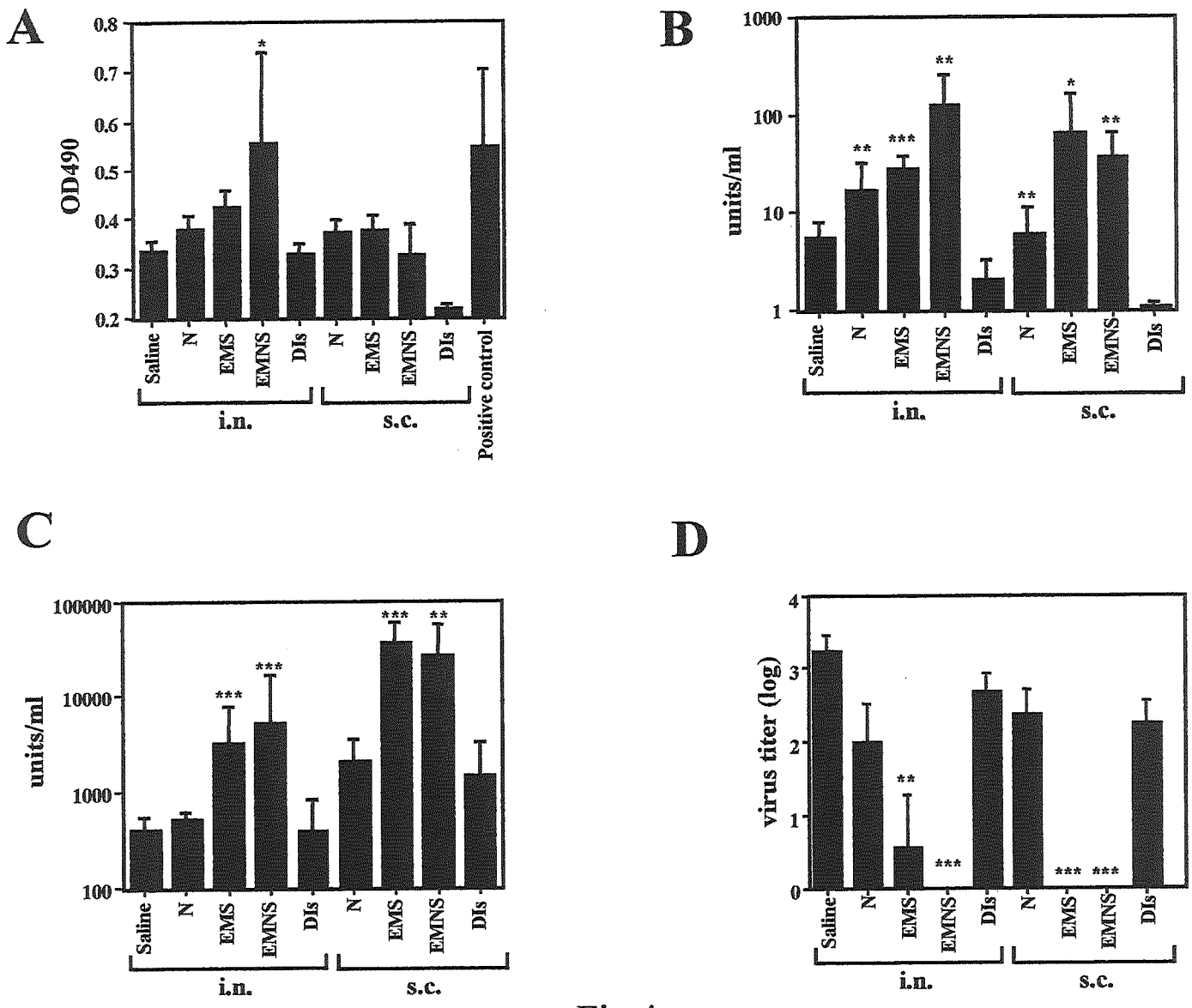
A
OD490
0.8
0.7
0.6
0.5
0.4
0.3
0.2
*
Saline
N
EMS
EMNS
DIs
N
EMS
EMNS
DIs
Positive control
i.n.
s.c.
B
units/ml
1000
100
10
1
**
***
**
*
**
**
Saline
N
EMS
EMNS
DIs
N
EMS
EMNS
DIs
i.n.
s.c.
C
units/ml
100000
10000
1000
100
***
***
***
**
Saline
N
EMS
EMNS
DIs
N
EMS
EMNS
DIs
i.n.
s.c.
D
virus titer (log)
4
3
2
1
0
**
***
***
***
Saline
N
EMS
EMNS
DIs
N
EMS
EMNS
DIs
i.n.
s.c.

Fig.4

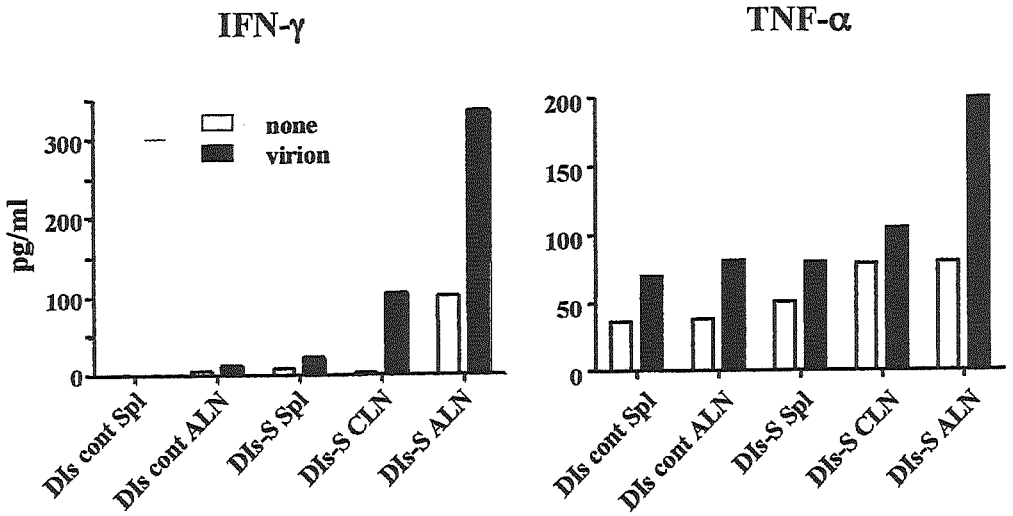
IFN-γ
TNF-α
none
virion
pg/ml
300
200
100
0
200
150
100
50
0
DIs cont Spl
DIs cont ALN
DIs-S Spl
DIs-S CLN
DIs-S ALN

Fig.5